

1 phylodyn: an R package for phylodynamic simulation 2 and inference 3

4 Michael D. Karcher^{1*}, Julia A. Palacios^{2,3*}, Shiwei Lan⁴, Vladimir N. Minin^{1,5}

5 ¹Department of Statistics, University of Washington, Seattle, WA, USA

6 ²Department of Statistics, Stanford University, Stanford, CA, USA

7 ³Department of Biomedical Data Science, Stanford University, Stanford, CA, USA

8 ⁴Department of Statistics, University of Warwick, Coventry, UK

9 ⁵Department of Biology, University of Washington, Seattle, WA, USA

10 **Abstract**

11 We introduce `phylodyn`, an R package for phylodynamic analysis based on gene
12 genealogies. The package main functionality is Bayesian nonparametric estimation of
13 effective population size fluctuations over time. Our implementation includes sev-
14 eral Markov chain Monte Carlo-based methods and an integrated nested Laplace
15 approximation-based approach for phylodynamic inference that have been developed
16 in recent years. Genealogical data describe the timed ancestral relationships of indi-
17 viduals sampled from a population of interest. Here, individuals are assumed to be
18 sampled at the same point in time (isochronous sampling) or at different points in
19 time (heterochronous sampling); in addition, sampling events can be modeled with
20 preferential sampling, which means that the intensity of sampling events is allowed
21 to depend on the effective population size trajectory. We assume the coalescent and
22 the sequentially Markov coalescent processes as generative models of genealogies. We

*The first two authors contributed equally to this paper.

23 include several coalescent simulation functions that are useful for testing our phylody-
24 namics methods via simulation studies. We compare the performance and outputs of
25 various methods implemented in `phylodyn` and outline their strengths and weaknesses.
26 R package `phylodyn` is available at <https://github.com/mdkarcher/phylodyn>.

27 **Introduction**

28 In the last several decades, phylodynamic inference has demonstrated its usefulness in ecol-
29 ogy and epidemiology [Grenfell et al., 2004, Holmes and Grenfell, 2009]. The key inferential
30 insight of phylodynamics is that population dynamics leave their mark in the shape of gene
31 genealogies and thereby the sequence data sampled. Kingman’s coalescent models the rela-
32 tionship between effective population size $N_e(t)$ and the likelihood of observing a particular
33 genealogy [Kingman, 1982]. In order to be computationally feasible, early coalescent-based
34 models required strong parametric assumptions on the effective population size trajectory
35 [Griffiths and Tavaré, 1994, Drummond et al., 2002, Kuhner et al., 1998]. More recently,
36 nonparametric models have allowed a much more diverse class of effective population size
37 trajectories to be inferred, at the cost of estimating many more parameters. Methods have
38 emerged that compromise between the two extremes, maintaining a tractable number of pa-
39 rameters while allowing for a diverse class of estimable trajectories [Drummond et al., 2005,
40 Minin et al., 2008, Palacios and Minin, 2013, Gill et al., 2013]. See the review by Ho and
41 Shapiro [2011] for a detailed comparison.

42 Here we unify user interfaces for three different but related Bayesian nonparametric

43 methods. These methods assume a log Gaussian process prior on $N_e(t)$. The first comes
44 from the work by Lan et al. [2015]. They implement a number of Markov chain Monte Carlo
45 (MCMC) algorithms for inferring effective population size trajectories from a fixed genealogy.
46 They compare different algorithms' computational efficiency and MCMC diagnostics.

47 The second methodology comes from the work by Palacios and Minin [2012] and Karcher
48 et al. [2016]. They target the same posterior as in [Lan et al., 2015], but implement an
49 integrated nested Laplace approximation (INLA) based approach. Utilizing INLA allows for
50 a significant computational speedup at the cost of only having access to the latent parameters'
51 approximate marginal distributions (as opposed to MCMC algorithms which approximate
52 the full joint distribution). Karcher et al. [2016] have an additional focus of accounting for
53 potential preferential sampling, which incorporates a likelihood relating the sampling times
54 of the genealogy to the effective population size trajectory.

55 The last methodology comes from the work by Palacios et al. [2015]. They implement
56 an MCMC algorithm for inferring effective population size trajectories from a sequence of
57 local genealogies. Here, genealogies are correlated and are assumed to be a realization of the
58 sequentially Markov coalescent (SMC') [Marjoram and Wall, 2006].

59 The R package `phylodyn` encapsulates all the above work. We integrated all of the above
60 methods in a unified user-friendly format, added detailed tutorials, included more features
61 such as simulation of genealogies from the coalescent model that accepts arbitrary but pos-
62 itive effective population size function [Palacios and Minin, 2013], and added features for
63 data manipulation and interaction with other data formats such as BEAST-XML [Drum-

mond et al., 2012]. These features greatly expand available phylodynamics methods in R. For example, the R package `ape` [Paradis et al., 2004] has a function `skyline` that implements the generalized skyline method for isochronous genealogies. To the best of our knowledge, no other R package infers effective population size trajectories from heterochronous genealogies. Other R packages for simulation of genealogical data exist (e.g. `phyclust` [Chen, 2011] and `ape`) but they are limited to very specific demographic scenarios such as piece-wise constant and exponential growth functions. Our addition of inference from a sequence of local genealogies expands the range of `phylodyn` to a broader class of models that have not been implemented in the previous versions of the package.

Functionality

Genealogical simulation

A genealogy is a rooted bifurcating tree with labeled tips. Branching events are called coalescent events which occur at coalescent times, and tips are located at sampling times. Given a vector of sampling times \mathbf{s} and an effective population size function $N_e(t)$, Kingman’s coalescent provides the following likelihood of observing a particular genealogy \mathbf{g} with coalescent times $\mathbf{t} = \{t_i\}_{i=2}^n$:

$$\Pr[\mathbf{g}|N_e(t), \mathbf{s}] \propto \prod_{k=2}^n \frac{C_{0,k}}{N_e(t_{k-1})} \exp \left[- \sum_{i=0}^{m_k} \int_{I_{i,k}} \frac{C_{i,k}}{N_e(t)} dt \right],$$

where $C_{i,k} = \binom{n_{i,k}}{2}$, $n_{i,k}$ is the number of lineages present during time interval $I_{i,k}$, and $I_{i,k}$ is a time interval defined by coalescent times and sampling times and $I_{0,k}$ is a time

82 interval that ends at coalescent time t_{k-1} . See [Lan et al., 2015] for notational details. The
83 `coalsim` function simulates coalescent times according to this distribution, given a vector of
84 sampling times and an arbitrary effective population size function `traj(t)`. The function
85 gives the option of using a time-transformation method or a thinning method for simulating
86 the coalescent times. The time-transformation method scales better but involves numerical
87 integration, while the thinning method is faster with small samples and is an exact method.
88 The `generate_newick` function takes the output generated with `coalsim` and returns the
89 corresponding genealogy in `ape`'s phylo format [Paradis et al., 2004]. We are not aware
90 of another R package that allows for simulating the coalescent process while allowing for
91 arbitrary sampling times as well as arbitrary positive effective population size trajectories.
92 `phylodyn` also provides functionality for easily simulating sampling times under preferential
93 sampling according to an arbitrary positive function f . The `pref_sample` function simulates
94 sampling times according to an inhomogeneous Poisson process with intensity $\lambda(t) = cf(t)^\beta$,
95 where parameters c and β control the expected number of sampled sequences and the strength
96 of preferential sampling, respectively. Currently the function only allows a thinning method,
97 but a time-transformation method is forthcoming.

98 **Markov chain Monte Carlo methods**

99 Following the approach of Gill et al. [2013] and Palacios and Minin [2012], Lan et al. [2015]
100 approximate $N_e(t)$ by a piece-wise linear function $N_f(t) = \sum_{d=1}^{D-1} \exp(f_d) 1_{(x_d, x_{d+1}]}$, defined
101 over a regular grid with end points $\mathbf{x} = \{x_d\}_{d=1}^D$, where x_1 equals the most recent sampling

102 time, and $x_D = t_2$, the time when the last two lineages coalesce. Hence, we seek to estimate
103 the posterior

$$\Pr[\mathbf{f}, \tau \mid \mathbf{g}] \propto \Pr[\mathbf{g} \mid \mathbf{f}] \Pr[\mathbf{f} \mid \tau] \Pr(\tau), \quad (1)$$

104 where $\Pr[\mathbf{g} \mid \mathbf{f}]$ is the coalescent likelihood, $\Pr[\mathbf{f} \mid \tau]$ is a Gaussian process prior on $\mathbf{f} =$
105 $\{f_d\}_{d=1}^{D-1}$ with precision τ , and $\Pr(\tau)$ is a Gamma hyperprior on τ . Our implementation
106 assumes a Gaussian process prior on \mathbf{f} with inverse covariance function $\mathbf{C}^{-1}(\tau) = \frac{1}{\tau} \mathbf{C}^{-1}$,
107 where \mathbf{C}^{-1} corresponds to a modified inverse covariance matrix of Brownian motion (see
108 [Lan et al., 2015] for details).

109 The `mcmc_sampling` function implements a variety of MCMC algorithms for estimating
110 the posterior (1), given the sufficient statistics for a genealogy (sampling times and coales-
111 cent times). Available methods are Hamiltonian Monte Carlo (HMC) [Duane et al., 1987,
112 Neal, 2011], split HMC [Leimkuhler and Reich, 2004, Neal, 2011, Shahbaba et al., 2014],
113 Metropolis-adjusted Langevin algorithm (MALA) [Roberts and Tweedie, 1996], adaptive
114 MALA [Knorr-Held and Rue, 2002], and Elliptical Slice Sampler (ESS) [Murray et al., 2010].
115 For a comparison of the computational efficiency of the different methods see [Lan et al.,
116 2015].

117 We illustrate `phylodyn`'s capabilities with a simulation example. We let $N_e(t)$ have
118 a seasonal boom-and-bust trajectory (provided by the `logistic_traj` function), and we
119 simulate a sequence of sampling times according to an inhomogeneous Poisson process with
120 intensity proportional to $N_e(t)$ using the `pref_sample` function. We simulate a genealogy
121 from the coalescent using the `coalsim` function, and supply it to the different sampling

122 algorithms of the `mcmc_sampling` function. We summarize the results in Figure 1.

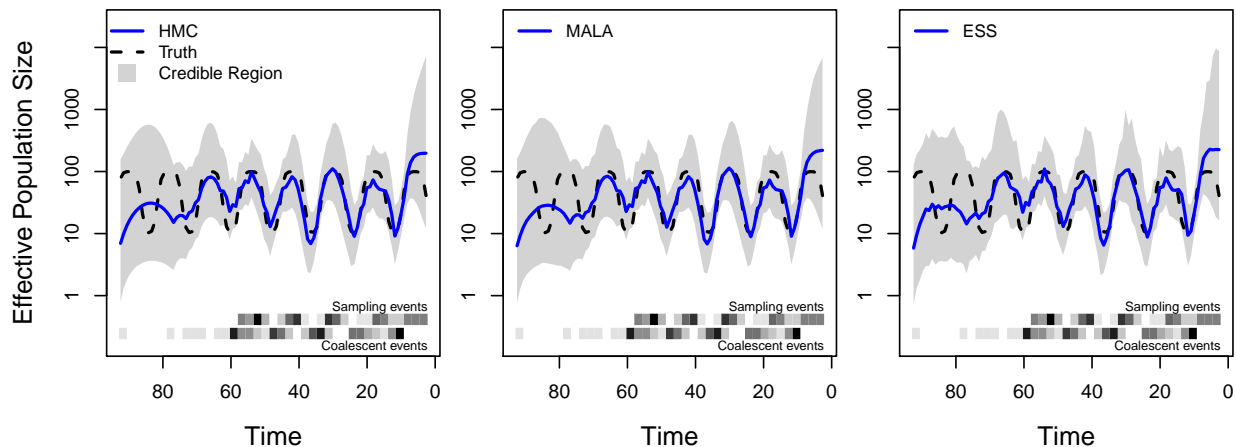


Figure 1: Seasonal boom-and-bust population size trajectory recovered with three different MCMC estimation methods: HMC, MALA and ESS. The dashed black lines represent the true population size trajectory. The solid blue lines represent the posterior median estimates, and the shaded regions represent the 95% credible regions. At bottom, the upper and lower heatmaps represent frequencies of sampling events and coalescent events, respectively. Time in simulated units of weeks.

123 Palacios et al. [2015] infer $N_e(t)$ from a sequence of m local genealogies under the SMC'
124 model [Marjoram and Wall, 2006]. The SMC' process is an approximation to the ancestral
125 recombination graph (ARG) which models the set of ancestral relationships and recombina-
126 tion events of multilocus sequences [Griffiths and Marjoram, 1997]. In our implementation,
127 we assume that our data consist of a sequence of genealogies that represent the ancestral
128 relationships at consecutive loci separated by recombination events. These consecutive ge-
129 nealogies are modeled as a continuous-time Markov chain along a chromosomal segment.

130 Here, we also approximate $N_e(t)$ by the piece-wise linear function $N_f(t)$ and rely on split
 131 HMC [Shahbaba et al., 2014] to sample from the posterior:

$$\Pr[\mathbf{f}, \tau \mid \mathbf{g}_0, \dots, \mathbf{g}_{m-1}] \propto \Pr[\mathbf{g}_0 \mid \mathbf{f}] \times \left\{ \prod_{i=0}^{m-2} \Pr[\mathbf{g}_{i+1} \mid \mathbf{g}_i, \mathbf{f}] \right\} \Pr[\mathbf{f} \mid \tau] \Pr(\tau), \quad (2)$$

132 where $\Pr[\mathbf{g}_0, \dots, \mathbf{g}_{m-1} \mid \mathbf{f}]$ is the sequentially Markov coalescent likelihood [Palacios et al.,
 133 2015]. Our `mcmc_smc` function samples from the posterior distribution (2). Figure 2 shows our
 134 estimate of $N_e(t)$ from 100 and 1000 local genealogies of $n = 20$ individuals simulated under
 135 a bottleneck demographic scenario. Palacios et al. [2015] show that our method recovers the
 136 bottleneck best when increasing the number of local genealogies.

SMC Inference of a Bottleneck

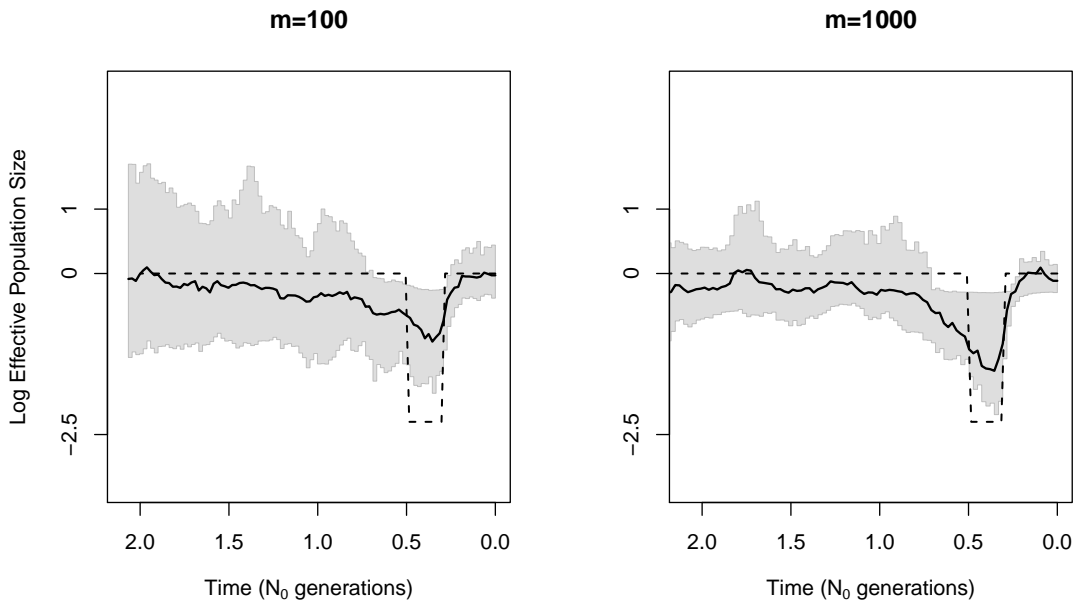


Figure 2: SMC' inference of $N_e(t)$ from $m = 100$ and $m = 1000$ simulated local genealogies of $n = 20$ individuals. The dashed black line represents the true population size trajectory, the solid black line represents the posterior median estimates, and the shaded regions represent the 95% credible regions. Estimation improves with larger number of genealogies.

137 **INLA-based methods**

138 We implement the INLA-based methods of Palacios and Minin [2012] and Karcher et al.
 139 [2016], using the same log-Gaussian prior on $N_e(t)$ as in the MCMC methods. The BNPR
 140 function implements the INLA approximation to obtain posterior medians and 95% Bayesian
 141 credible intervals (BCIs) of $N_f(t)$. Being a numerical approximation, this method runs ex-
 142 tremely quickly. However, the method only estimates the marginals of the posterior of the
 143 effective population size and hyperparameters, rather than the full joint posterior distri-
 144 bution of MCMC-based methods. This is frequently sufficient for most purposes involving
 145 phylodynamic inference, but offers significant improvement in computational efficiency.

146 We also implement the BNPR-PS method of Karcher et al. [2016]. In cases where the
 147 frequency of sampling times is related to effective population size, including a sampling
 148 time model provides additional accuracy and precision. We model the sampling times as
 149 an inhomogeneous Poisson process with intensity proportional to a power of the effective
 150 population size, with the following log-likelihood:

$$\log[\Pr(\mathbf{s} \mid \mathbf{f}, \beta_0, \beta_1)] = C + n\beta_0 + \sum_{i=1}^n \beta_1 \log[N_f(s_i)] - \int_{s_m}^{s_0} \exp(\beta_0)[N_f(r)]^{\beta_1} dr.$$

151 This leads to the posterior that conditions on both coalescent and sampling times:

$$\Pr[\mathbf{f}, \tau, \beta_0, \beta_1 \mid \mathbf{g}, \mathbf{s}] \propto \Pr[\mathbf{g} \mid \mathbf{s}, \mathbf{f}] \Pr[\mathbf{s} \mid \mathbf{f}, \boldsymbol{\beta}] \Pr[\mathbf{f} \mid \tau] \Pr(\tau) \Pr(\beta_0, \beta_1). \quad (3)$$

152 To illustrate, we use the same genealogy under seasonal boom-and-bust population size
 153 trajectory as in Figure 1. We apply BNPR and BNPR-PS to this genealogy, and summarize
 154 the results in Figure 3. Since our sampling times and genealogy were simulated with pref-

155 erential sampling, we notice improved performance from BNPR-PS, which correctly models
156 the sampling times.

157 Discussion

158 Phylodynamic inference aims to enhance our understanding of infectious disease dynamics
159 that involves a combination of evolutionary, epidemiological, and immunological processes
160 [Grenfell et al., 2004]. Although phylodynamic methods have been developed and success-
161 fully employed over the last 15 years, there are still many challenges in extending these
162 methods to incorporate different types of information and evolutionary complexities of cer-
163 tain pathogens [Frost et al., 2015]. The tools developed in `phylodyn` currently concentrate on
164 estimation of population dynamics from genealogical and sampling information — a subset
165 of phylodynamics problems. Phylodynamic inference from sequence data alone is challeng-
166 ing because the state spaces of genealogies \mathbf{g} and effective population size trajectories $N_e(t)$
167 are large. The MCMC tools implemented in `phylodyn` allow for an efficient exploration of
168 the state space of effective population size trajectories $N_e(t)$ when either a single genealogy
169 is available or multiple local sequential genealogies are available. Future implementation in
170 `phylodyn` will involve the exploration of the joint space of genealogies, population size trajec-
171 tories and other epidemiological processes. We envision that the increasing popularity of R
172 will allow researchers to integrate different packages with `phylodyn`. For instance, `phylodyn`
173 can be used in combination with the R package `coalescentMCMC` to account for genealogical
174 uncertainty. In addition, our coalescent simulation functions should be of interest to a wide

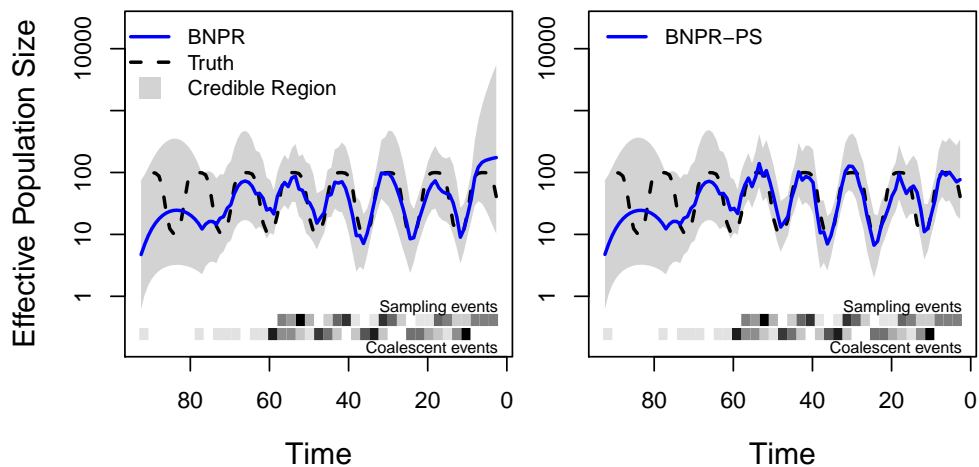


Figure 3: Graphical representation of the output of a single genealogy simulation and different BNPR estimation methods. The dashed black lines represent the true population size trajectory. The solid blue lines represent the posterior median estimates, and the shaded regions represent the 95% credible regions. The bottom upper and lower heatmaps represent frequencies of sampling events and coalescent events, respectively. For this figure, we sampled individuals according to an inhomogeneous Poisson process with intensity proportional to effective population size $N_e(t)$ ($\beta_1 = 1$). The plot on the left is generated by Bayesian nonparametric phylodynamic reconstruction (BNPR) that does not account for preferential sampling, while the plot on the right is generated by Bayesian nonparametric phylodynamic reconstruction with preferential sampling (BNPR-PS) and incorporates our sampling time model. Time is in months.

175 range of users of the coalescent.

176 **Acknowledgments**

177 We thank the reviewers and associate editor for their constructive criticism that greatly
178 improved the manuscript. M.D.K. and V.N.M. were supported by the NIH grant U54
179 GM111274. V.N.M. was supported by the NIH grant R01 AI107034.

180 **References**

- 181 W.C. Chen. Overlapping Codon Model, Phylogenetic Clustering, and Alternative Partial
182 Expectation Conditional Maximization Algorithm, 2011. URL <http://gradworks.umi.com/34/73/3473002.html>.
183
- 184 A. J. Drummond, G. K. Nicholls, A. G. Rodrigo, and W. Solomon. Estimating mutation
185 parameters, population history and genealogy simultaneously from temporally spaced se-
186 quence data. Genetics, 161(3):1307–1320, 2002.
- 187 A. J. Drummond, A. Rambaut, B. Shapiro, and O. G. Pybus. Bayesian coalescent inference
188 of past population dynamics from molecular sequences. Molecular Biology and Evolution,
189 22(5):1185–1192, 2005.
- 190 A. J. Drummond, M. A. Suchard, D. Xie, and A. Rambaut. Bayesian phylogenetics with
191 BEAUti and the BEAST 1.7. Molecular Biology and Evolution, 29:1969–1973, 2012.

192 S. Duane, A. D. Kennedy, B. J. Pendleton, and D. Roweth. Hybrid Monte Carlo. Physics
193 letters B, 195(2):216–222, 1987.

194 Simon D W Frost, Oliver G Pybus, Julia R Gog, Cecile Viboud, Sebastian Bonhoeffer, and
195 Trevor Bedford. Eight challenges in phylodynamic inference. Epidemics, 10:88–92, March
196 2015.

197 M. S. Gill, P. Lemey, N. R. Faria, A. Rambaut, B. Shapiro, and M. A. Suchard. Improv-
198 ing Bayesian population dynamics inference: a coalescent-based model for multiple loci.
199 Molecular Biology and Evolution, 30(3):713–724, 2013.

200 B. T. Grenfell, O. G. Pybus, J. R. Gog, J. L. N. Wood, J. M. Daly, J. A. Mumford, and E. C.
201 Holmes. Unifying the epidemiological and evolutionary dynamics of pathogens. Science,
202 303(5656):327–332, 2004.

203 R. C. Griffiths and S. Tavaré. Sampling theory for neutral alleles in a varying environment.
204 Philosophical Transactions of the Royal Society of London. Series B: Biological Sciences,
205 344(1310):403–410, 1994.

206 R.C. Griffiths and P. Marjoram. An ancestral recombination graph. In Peter Donnelly and
207 Simon Tavaré, editors, Progress in population genetics and human evolution, volume 87 of
208 IMA Volumes in Mathematics and Its Applications, pages 257–270. Springer Verlag, New
209 York, 1997.

210 S. Y. W. Ho and B. Shapiro. Skyline-plot methods for estimating demographic history from
211 nucleotide sequences. Molecular Ecology Resources, 11(3):423–434, 2011.

212 E. C. Holmes and B. T. Grenfell. Discovering the phylodynamics of RNA viruses. PLoS
213 Computational Biology, 5(10):e1000505, 2009.

214 M. D. Karcher, J. A. Palacios, T. Bedford, M. A. Suchard, and V. N. Minin. Quantify-
215 ing and mitigating the effect of preferential sampling on phylodynamic inference. PLoS
216 Computational Biology, 12:e1004789, 2016.

217 J. F. C. Kingman. The coalescent. Stochastic Processes and Their Applications, 13(3):
218 235–248, 1982.

219 Ll Knorr-Held and H. Rue. On block updating in Markov random field models for disease
220 mapping. Scandinavian Journal of Statistics, 29(4):597–614, 2002.

221 M. K. Kuhner, J. Yamato, and J. Felsenstein. Maximum likelihood estimation of population
222 growth rates based on the coalescent. Genetics, 149(1):429–434, 1998.

223 S. Lan, J. A. Palacios, M. D. Karcher, V. N. Minin, and B. Shahbaba. An efficient Bayesian
224 inference framework for coalescent-based nonparametric phylodynamics. Bioinformatics,
225 31:3282–3289, 2015.

226 B. Leimkuhler and S. Reich. Simulating Hamiltonian dynamics, volume 14. Cambridge
227 University Press, 2004.

228 P. Marjoram and J. Wall. Fast “coalescent” simulation. BMC Genetics, 7(1), 2006.

229 V. N. Minin, E. W. Bloomquist, and M. A. Suchard. Smooth skyride through a rough

230 skyline: Bayesian coalescent-based inference of population dynamics. Molecular Biology
231 and Evolution, 25(7):1459–1471, 2008.

232 I. Murray, R.P. Adams, and D. Mackay. Elliptical slice sampling. In International Conference
233 on Artificial Intelligence and Statistics, pages 541–548, 2010.

234 R. M. Neal. MCMC using Hamiltonian dynamics. In S. Brooks, A. Gelman, G. Jones, and
235 X.L. Meng, editors, Handbook of Markov Chain Monte Carlo, pages 113–162. CRC Press,
236 2011.

237 J. A. Palacios and V. N. Minin. Integrated nested Laplace approximation for Bayesian non-
238 parametric phylodynamics. In Proceedings of the Twenty-Eighth International Conference
239 on Uncertainty in Artificial Intelligence, pages 726–735, 2012.

240 J. A. Palacios and V. N. Minin. Gaussian process-based Bayesian nonparametric inference
241 of population size trajectories from gene genealogies. Biometrics, 69(1):8–18, 2013.

242 J. A. Palacios, J. Wakeley, and S. Ramachandran. Bayesian nonparametric inference of
243 population size changes from sequential genealogies. Genetics, page 115, 2015.

244 E. Paradis, J. Claude, and K. Strimmer. APE: analyses of phylogenetics and evolution in R
245 language. Bioinformatics, 20:289–290, 2004.

246 G. O. Roberts and R. L. Tweedie. Exponential convergence of Langevin distributions and
247 their discrete approximations. Bernoulli, pages 341–363, 1996.

248 B. Shahbaba, S. Lan, W. O. Johnson, and R. M. Neal. Split Hamiltonian Monte Carlo.
249 Statistics and Computing, 24(3):339–349, 2014.

250 **Data Accessibility**

251 `phylodyn` is available at <https://github.com/mdkarcher/phylodyn>. Installation instruc-
252 tions are provided in the README file. Several vignettes have been included to walk users
253 through the standard workflow, as well as a number of example datasets from the papers
254 that introduced the methods included in the R package.